NASA Technical Memorandum 104490

Sliding Wear of Self-Mated Al_2O_3-SiC Whisker Reinforced Composites at 23-1200 °C

Serene C. Farmer
Lewis Research Center
Cleveland, Ohio

Patricia O. Book
Cleveland State University
Cleveland, Ohio

and

Christopher DellaCorte
Lewis Research Center
Cleveland, Ohio

July 1991

NASA

SLIDING WEAR OF SELF-MATED Al_2O_3-SIC WHISKER REINFORCED COMPOSITES AT 23 TO 1200 °C

Serene C. Farmer
National Aeronautics and Space Administration
Lewis Research Center
Cleveland, Ohio 44135

Patricia O. Book*
Cleveland State University
Cleveland, Ohio 44115

and

Christopher DellaCorte
National Aeronautics and Space Administration
Lewis Research Center
Cleveland, Ohio 44135

ABSTRACT

Microstructural changes occurring during sliding wear of self-mated Al_2O_3-SiC whisker reinforced composites were studied using optical, scanning electron microscopy, and transmission electron microscopy. Pin-on-disk specimens were slid in air at 2.7 m/sec sliding velocity under a 26.5 N load for 1 hr. Wear tests were conducted at 23, 600, 800, and 1200 °C. Mild wear with a wear factor of 2.4×10^{-7} to 1.5×10^{-6} mm^3/Nm was experienced at all test temperatures.

The composite shows evidence of wear by fatigue mechanisms at 800 °C and below. Tribochemical reaction (SiC oxidation and reaction of SiO_2 and Al_2O_3) leads to intergranular failure at 1200 °C. Distinct microstructural differences existing at each test temperature are reported.

---

*Resident Research Associate at NASA Lewis Research Center.

1. Introduction

The addition of SiC whiskers to ceramic matrices has been demonstrated to enhance the material's toughness as compared to the monolith. In SiC whisker reinforced alumina, significant increases in toughness without sacrificing strength have been obtained. The good mechanical properties of the alumina composites combined with favorable oxidation resistance has fostered continued interest in SiC whisker reinforced alumina for use in heat engines and as cutting tools.

Since improved fracture toughness can mean improved wear resistance, the potential application of alumina composite materials in high temperature sliding components is subject to ongoing investigation. Extensive research on the wear of self-mated SiC whisker reinforced alumina has been conducted by Yust, Leitmaker, and Devore [1] and Yust and Allard [2] at temperatures up to 800° C in both nitrogen and air environments.

Their results of pin-on-disk sliding experiments with alumina composites show a 2 to 4 order of magnitude improvement in wear as compared to monolithic alumina. The composite wears by fracture, producing wear particles 10 to 40 nm in diameter. Testing results obtained in air were similar to tests in nitrogen except at the highest temperature, 800 °C. Composite material tested at 800 °C in air developed an oxidation layer on the rubbing surface. Reduced wear was experienced. Using Auger and EDS x-ray analysis, Yust and Allard determined that the surface layer was predominantly a mixture of Al_2O_3 and SiO_2. Transmission electron microscopy revealed subsurface dislocations not observed in specimens tested at lower temperatures.

NASA has undertaken a research program to extend study of the wear behavior of SiC whisker reinforced Al_2O_3 composites to temperatures as high as 1200 °C in air. We

concentrated on examination of the surface and near-surface microstructural changes which occur at elevated temperatures, rather than the generated debris, as this facet of the wear problem has been less studied.

Self-mated pin-on-disk wear tests were performed at room temperature, 600, 800, and 1200 °C. The pin wear surface was then examined by scanning electron microscopy (SEM). Transmission electron microscopy (TEM) was employed to identify the microstructural changes which accompany wear at high temperatures.

2. Experimental Procedure

The composite material used in our experiments was hot pressed high purity alumina powder (>99.5 percent purity) containing 25 vol. % Tateho SiC whiskers. The composite was supplied by Arco Products, Greer, SC. During hot pressing, the whiskers preferentially align perpendicular to the pressing direction. The alumina grain size is ~2 μm and the predominant defects are large whisker free regions and voids several microns in diameter. These defects are visible in optical micrographs of polished cross-sections, Fig. 1.

Pins were fabricated such that the long axis of the pin is in the hot press direction. Thus the whiskers are aligned within the rubbing surface of the pin. The pins are 0.476 cm in diameter by 2.5 cm. A 2.54 cm radius is machined onto the pin end and diamond polished to ~0.1 μm rms surface finish. The wear discs are 6.35 cm in diameter and 1.25 cm thick with their flat faces diamond polished to ~0.1 μm rms surface finish.

Specimens were tested in a high temperature tribometer at a sliding speed of 2.7 m/sec (1000 rpm) for one hour; a total sliding distance of 9.7 km. The normal load was 26.5 N. The rig has a SiC glowbar furnace which was heated 600 °C/hr to the test temperature and shut off to cool down. All tests were run in air with relative humidity from 40 to 65 percent

at 23 °C. Pin wear measurements were made by measuring the size of the flat and calculating the volume of material displaced.

In the microstructural analysis presented here, the flat worn on the pin was examined in a Cambridge 200 scanning electron microscope equipped with a Princeton Gamma Tech (PGT) energy dispersive spectrometer. Specimens for transmission electron microscopy were made by cutting a 3 mm disk from the pin wear scar. To preserve the wear surface, specimens were then polished and ion beam milled from the opposing side to perforation. Specimens were examined on a Philips 400T equipped with an ultra thin window Kevex energy dispersive spectrometer.

3. Results

The results of the friction and wear experiments are summarized in Fig. 2. Mild wear, wear factor 2.4×10^{-7} to 1.5×10^{-6} mm^3/Nm, occurred at all temperatures (23, 600, 800, and 1200 °C). Further details of the tribometer and tribological data on these materials have been previously reported [3,4]. Although wear increases a factor of ~5 at elevated temperatures, the increase is not monotonic. The measured wear factor was a maximum at 600 °C. A slight abatement in wear factor was measured at 800 °C. Distinct microstructural differences exist at each test temperature. These differences are discussed below.

3.1. *Wear at 23 °C*

An SEM image of the pin wear flat is shown in Fig. 3(a). The foreground is the unworn pin hemisphere. There is a ridge of compacted debris, ~5 μm high at its maximum accumulation, where the wear flat begins. Details of the debris in the flat are seen in Fig. 3(b). Debris particles are equiaxed and particles ~1 to 5 μm in diameter were measured. Examined in TEM [4], the debris is seen to consist of alumina and SiC particles 0.2 to 0.5 μm in size

having sharp fracture faces, Fig. 3(c). In a detailed study of debris, Yust et al. determined that debris particles visible in SEM were actually agglomerates of much smaller particles, many less than 1 μm. These authors identified the ~0.1 μm particles as being of the magnitude of asperity contacts which once removed are easily bonded by compressive forces. Particles agglomerate and compress to form an adherent layer. We observe considerable agglomeration consistent with Yust's interpretation.

A typical TEM micrograph of the near surface region appears in Fig. 4. The alumina grains are largely free of dislocations and in general do not contain pores. (The occasional dislocation is seen adjacent to a whisker when the whisker is located intragranularly). The whiskers are heavily faulted and contain impurity inclusions concentrated in the whisker central region. Impurities in Tateho whiskers used in this material and other commercially available whiskers have been characterized by Nutt and others [5-7]. The main metallic impurities in Tateho whiskers in parts per million are 3000 ppm Ca, 2400 ppm Mn, 1300 ppm Al, 800 ppm Mg, and 500 ppm Fe.

Glassy phase at the two-grain boundaries between alumina grains is limited. However glass is found at all triple points and at whisker agglomerates. In general, glass in Al_2O_3-SiC whisker composites arises in part from sintering aids and in part from oxidation of SiC during grinding and composite fabrication [8]. Sintering aids, however, were not used in the processing of this material. Thus the glass present derives predominantly from the added whiskers. (Also present in some intergranular regions of this material are iron silicide inclusions. The Fe is believed to originate from the steel media used in ball milling powders. EDS analysis of such particles reveals the high Fe content and associated steel alloying elements Cr, Mn, and V.)

Both intra- and intergranular cracking of the alumina was observed. Some deflection of the crack along the whisker also occurs, Fig. 4. Crack deflection has been decribed as the dominant low temperature mechanism contributing to increased toughness [7].

3.2. *Wear at 600 °C*

Material is removed by brittle fracture as at lower temperatures. Fig. 6 shows a region >10 μm in extent where material has been removed by massive intergranular fracture. Whiskers have clearly debonded and been pulled out. The fractured area is surrounded by and partially obscured by compacted debris. Directional smearing of the compacted debris is pronounced at elevated temperatures, Fig. 7(a). The compacted layer is soft relative to freshly generated debris and groove and lip formation occurs, Fig. 7(b). The ridge between the pin wear flat and the unworn hemispherical surface of the pin is shown in Fig. 8(a). In addition to individual wear particles, larger agglomerates of wear particles several microns in diameter and wear debris rolls are observed. The latter can be more clearly seen in the enlargement, Fig. 8(b). We believe most of the wear debris rolls are whisker material plus other compacted and adhered debris.

TEM images of the 600 °C wear surface showed severe microcracking. A high dislocation density was invariably found in microcracked regions. (See Fig. 9.) Grains further removed from the microcracked regions contained few if any dislocations.

3.3. *Wear at 800 °C*

Although the measured wear factor was lower at 800 °C than at 600 °C, the wear surface as observed in SEM appeared very similar to the 600 °C sample. The compacted debris largely obscures the underlying surface. The debris agglomerates were larger than produced during 600 °C ambient temperature wear and somewhat more rounded. Wear debris rolls were again

observed of similar diameter and length, 0.5 to 2.5 μm diameter and 10 μm or less in length, Fig. 10.

Numerous microstructural changes are evident in TEM. The first is the occurrence of a layer of fine mullite crystals, ~100 nm diameter, in an aluminosilicate glass, Fig. 11. Mullite formation is limited in extent and is present at a concentration too low for detection in conventional x-ray diffractometry. Alumina grains bounded by glass are facetted. Note that dislocations are visible albeit in poor contrast in the Al_2O_3 grain. Dislocation density at the wear surface was high as was observed at 600 °C.

The most striking microstructural difference observed at the higher temperature is crack healing, Fig. 12(a) and (b). The material appears to have extensively microcracked followed by crack healing. The healed cracks eventually form arrays of pores. Fig. 12(a) shows the early stages of crack healing. Fig. 12(b) is a later stage where a healed crack is now evidenced by a row of pores. Many pores are facetted and many contain impurity particles introduced from the wear surface and environment. Most frequently observed crystalline impurities contain Zn, Cu, Zr, or Pb. (The Zr is most likely from the zirconia furnace lining. The other elements suggest a leaded brass or bronze but no effort was made to identify a specific source.)

Regions containing healed microcracks invariably have dislocations visible under the appropriate diffraction conditions. In addition to microcracks, healed cracks, and dislocations, twinning was observed in a few grains, Fig. 13. Even at elevated temperatures, the microstructural changes observed were quite surface specific. Grains which were further away from the sliding interface (~1 mm) appear unaffected.

3.4. *Wear at 1200 °C*

At the highest test temperature, large smears of material are visible at the leading and trailing edges of the wear flat. The ridge between accumulated debris and the hemispherical surface of the pin consists of a complex mat of glass, mullite, debris particles, and whiskers, Fig. 14(a) and b. Debris that is thrown free of the wear scar area adheres to the pin surface and can be seen in the foreground of Fig. 14(a). Detail of debris near the compacted ridge appears in Fig. 14(c). Small particles a few microns in diameter and larger agglomerates and compacted flakes are visible. The amount of wear debris rolls has greatly increased. The length of the rolls has increased significantly. Lengths between 20 and 30 μm are now common.

Energy dispersive spectroscopy (EDS) confirms that much of the wear roll debris are whiskers. Extensive debonding of whiskers and their ejection from the sliding surface is indicated by the long lengths of such debris (up to 55 μm). Measured diameters range form 1 to 4 μm. The diameters are significantly greater than expected whisker diameters indicating that adhered alumina-rich debris coats the whisker surface.

Oxidation of SiC whiskers and the resulting microstructural changes become apparent in TEM. The oxidation of SiC whiskers in Al_2O_3 matrix composites and subsequent precipitation of mullite has been effectively studied using high resolution electron microscopy by Lin, Marieb, Morrone, and Nutt [9]. The glass penetrates along alumina grain boundaries and reacts with the alumina. Mullite precipitates from the resulting aluminosilicate glass. The penetration of glass along alumina grain boundaries, facetting of alumina grains during alumina dissolution, and subsequent mullite precipitation produces the microstructure shown in Fig. 15(a) and (b). Large regions of mullite and aluminosilicate glass exist at the surface of

the 1200 °C sample, Fig. 14(b). Mullite formation occurs at levels detectable in x-ray diffractometry.

In sharp contrast to the 600 and 800 °C samples, dislocations were not commonly observed nor was extensive microcracking in evidence. The effects of SiC whisker oxidation (Al_2O_3 dissolution, mullite precipitation, and whisker debonding) dominate the microstructural changes during wear at 1200 °C.

4. Discussion

The 23 °C wear sample wore by microfracture and did not exhibit other microstructural changes. Microstructural changes observed during sliding wear at elevated test temperatures, e.g. oxidation and crack healing, are well known high temperature phenomena. Their subsequent effect on mechanical properties has been investigated [13-16].

During sliding wear, local temperature elevation through frictional heating induces microstructure changes not generally associated with the ambient test temperatures. Griffioen et al. [10] observed hot-spots in unlubricated sliding surfaces and described the contact regions experiencing frictional heating as being of varied dimensions and greatly elevated temperature. In previous work, Dellacorte [11] used the model of Ashby [12] to estimate the degree of temperature elevation in pin-on-disk sliding wear. Even at moderate loads and speeds, the frictional temperatures are estimated to rise above the ambient by 400 to 500 °C.

The most prominent microstructural changes we observed in sliding wear of Al_2O_3-SiC whiskers composite: dislocation activity, crack healing, and SiC oxidation are discussed below.

4.1. *Dislocation activity*

Wear at room temperature appears to proceed from crack initiation and growth. Few dislocations are observed. In contrast, wear at 600 °C and 800 °C produced massive fracture. Analysis of the dislocations generated show they arise from basal slip, <1120>(0001). There is no indication of other active slip systems.

To satisfy von Mises' criterion for yield, five independent slip systems need be activated. Unable to deform by the conservative motion of dislocations, the material microcracks. The extension and linkage of microcracks is believed to lead to the massive fracture observed.

Contrary to initial expectations, dislocation activity was most prevalent at the intermediate ambient test temperatures of 600 and 800 °C. At the highest ambient temperature used in our studies, 1200 °C, the oxidation of whiskers initiates a series of unfavorable chemical reactions. The material fails intergranularly without generating the high stresses that can initiate dislocation activity.

4.2. *SiC oxidation*

Oxidation of SiC has been reported at temperatures as low as 800 °C [13] and was identified in previous 800 °C wear studies [2]. Linear oxidation rates were reported at the low temperatures. Parabolic kinetics are observed at high temperatures (>1200 °C) where a protective SiO_2 layer forms. Oxidation in both temperature regimes is restricted to the surface regions. Where oxidation occurs, a significant increase in the incidence of whisker pullout has been reported [14].

The glass formed during SiC oxidation penetrates boundaries reacting with the alumina grains. We observe that the SiO_2 glass formed during sliding wear at 800 and 1200 °C

contains small amounts of Ca, presumably from the whiskers, and a trace of Na, a common impurity in high grade alumina. These impurities lower the viscosity of the glass. The oxidation of SiC whiskers and subsequent reaction of the SiO_2 produced with the surrounding alumina grains facilitates extensive debonding of the whiskers during wear. Differences in thermal expansion coefficients has been advanced as a contributing factor [11].

Although SiC oxidation is not unanticipated during 800 °C wear, the formation of mullite at such low temperatures has not been reported. The eutectic in the Al_2O_3-SiO_2 binary system occurs at 1550 °C. Impurities substantially lower the liquidus temperature. Formation of mullite is common with many mixtures containing SiO_2 and Al_2O_3 (glazes) when fired above 1300 to 1350 °C. In isothermal aging of as-received composite material, mullite was detected at similar temperatures i.e. 1300 °C. At the isolated regions of mullite plus glass found at the 800 °C wear surface, Ca and Fe were detected. The presence of impurities and the calculated temperature increase from frictional heating of 400 to 500 °C appear to adequately explain mullite formation at the 800 °C ambient temperature. At a higher ambient wear temperature, 1200 °C, the reaction is no longer localized to Fe containing regions.

4.3. *Crack healing*

Strengthening of alumina and other ceramics through crack healing has been studied at temperatures of 1400 °C and above [15-17]. Crack healing causes substantial strength recovery in thermal-shocked materials [17]. Under the conditions of frictional heating and applied pressure experienced during wear, we can observe crack healing at much lower ambient temperatures and within short times (1 hr). Crack healing proceeds through several well defined steps: (1) pinching of cracks, (2) cracks assume the shape of cylindrical voids, (3) cylindrical voids breakup into numerous spherical pores.

Both glass formation through SiC oxidation and crack healing are evident in the 800 °C wear samples. Further study is needed to determine the extent to which these or other mechanisms contribute to the wear abatement at 800 °C.

4.4. *Remarks*

In the tests conducted, mild wear was experienced at all temperatures (23, 600, 800, and 1200 °C). We have examined microstructural changes which occur at elevated temperature and find they exert only a factor of ~5 change in wear rate with temperature for these very short times (1 hr). Several issues are of interest for future work. These include studies of: (1) wear at elevated temperatures for extended times, (2) wear at temperatures between 23 and 600 °C (Yust et al. reported severe wear at 400 °C before a return to mild wear at 800 °C.) and (3) effect of varying amounts of impurities which affect liquidus temperatures, glass softening, and glass viscosity.

5. Results and Conclusions

Al_2O_3-SiC whisker reinforced material was wear tested at 2.7 m/sec sliding velocity under 26.N load for 1 hr at temperatures of 23, 600, 800, and 1200 °C. The following results and conclusions were obtained:

1. Al_2O_3-SiC whisker reinforced composites appear a promising high temperature wear material. Mild wear, wear factor 2.4×10^{-7} to 1.5×10^{-6} mm^3/Nm, was observed during sliding wear of self-mated Al_2O_3-SiC whisker reinforced pin-on-disk specimens tested over the temperature range 23 to 1200 °C. Wear rates generally increased with temperature but at all temperatures were about an order of magnitude better than reported for sliding wear of monolithic Al_2O_3.

2. The wear of these materials is dominated by microfracture at low ambient temperatures, 23 and 600 °C.

3. The frictional heating experienced during pin-on-disk wear induces extensive microstructural changes not otherwise observed at the ambient test temperatures. Whisker oxidation, the associated glass penetration of the alumina grain boundaries, and whisker debonding control wear at 1200 °C. A more complex combination of mechanisms contribute to wear at the intermediate temperature of 800 °C.

4. While wear rates generally increase at elevated temperatures, there is a possible abatement in wear rate at ~800 °C where both glass formation through SiC oxidation and crack healing are evident.

5. Although wear rates remain favorably low at elevated temperature over test times of 1 hr, microstructural changes occur which may have significant effect on the wear properties over extended time and need be considered.

References

1. C.S. YUST, J.M. LEITNAKER, and C.E. DEVORE, Wear **122** (1988) 151.
2. C.S. YUST and L.F. ALLARD, Tribology Trans. **32** (1989) 331.
3. H.E. SLINEY and C. DELLACORTE, NASA TM-102405 (1989).
4. C. DELLACORTE, S.C. FARMER, and P.O. BOOK, NASA TM-102549 and "Tribology of Composite Materials," ASM (1990) 345.
5. S.R. NUTT, J. Am. Ceram. Soc. **71** (1988) 149.
6. K.R. KARASEK, S.A. BRADLEY, J.T. DONNER, M.R. MARTIN, K.L. HAYNES, and H.C. YEH, J. Mater. Sci. **24** (1989) 1617.
7. J. HOMENY, W.L. VAUGHN, and M.K. FERBER, J. Am. Ceram. Soc. **73** (1990) 394.

8. M. FALK and S. KARUNANITHY, Mater. Sci. Eng. A., **114** (1989) 209.

9. F. LIN, T. MARIEB, A. MORRONE, and S. NUTT, in High Temperature/High Performance Composites, edited by F.D. Lemkey et al., MRS Symp. Proc. Vol. 120, (Materials Research Society), Pittsburgh, 1988, p. 323.

10. J.A. GRIFFIOEN, S. BAIR and W.O. WINER, in Mechanisms and Surface Distress, Proc. 12th Leeds-Lyon Symposium, edited by D. Dowson, C.M. Taylor, M.Godet and D. Berthe, (Butterworths, London, 1986), p. 238.

11. C. DELLACORTE, NASA TM-103799 (1991).

12. M.F. ASHBY, in Proceedings of Int. Workshop on Wear Modelling, Argonne Nat. Lab., June 1988, edited by F.A. Nichols, A.E. Michael, and L.A. Northcutt (1988) p. 25.

13. S.R. NUTT, P. LIPETZKY, and P.F. BECHER, Mater. Sci. Eng. A **126** (1990) 165.

14. P.F. BECHER, P. ANGELINI, W.H. WARWICK, and T.N. TIEGS, J. Am. Ceram. Soc. **73** (1990) 91.

15. T.K. GUPTA, in Structure and Properties of MgO and Al_2O_3 Ceramics, edited by W.D. Kingery, Advances in Ceramics, Vol. 10, (American Ceramic Society, Columbus, OH; 1984) p. 750.

16. T.K. GUPTA, J. Am. Ceram. Soc. **59** (1976) 259.

17. T.K. GUPTA, J. Am. Ceram. Soc. **61** (1978) 191.

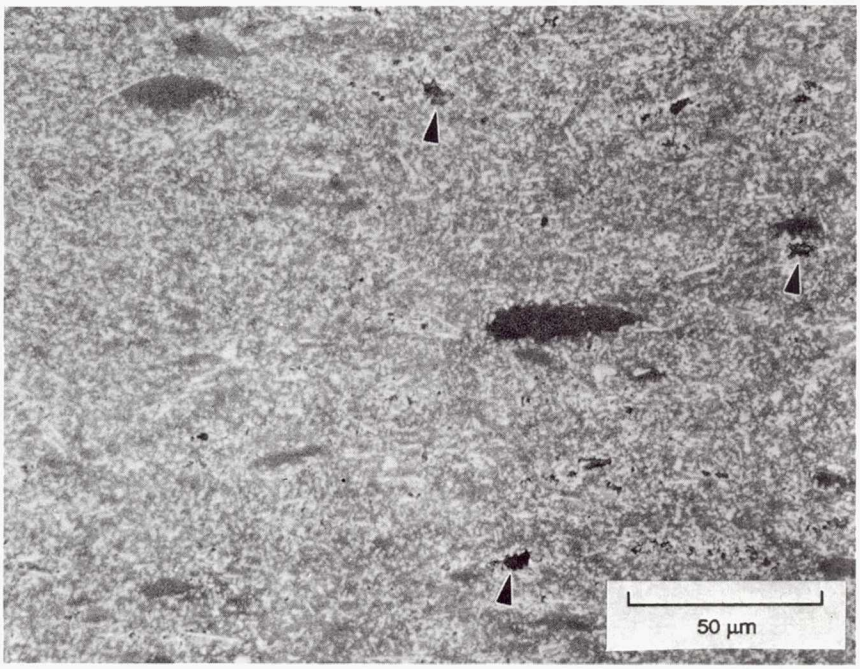

Figure 1.—Optical micrograph of Al_2O_3-SiC whisker pin. Several large whisker-free regions are visible (whiskers appear white). A few of the larger voids are arrowed.

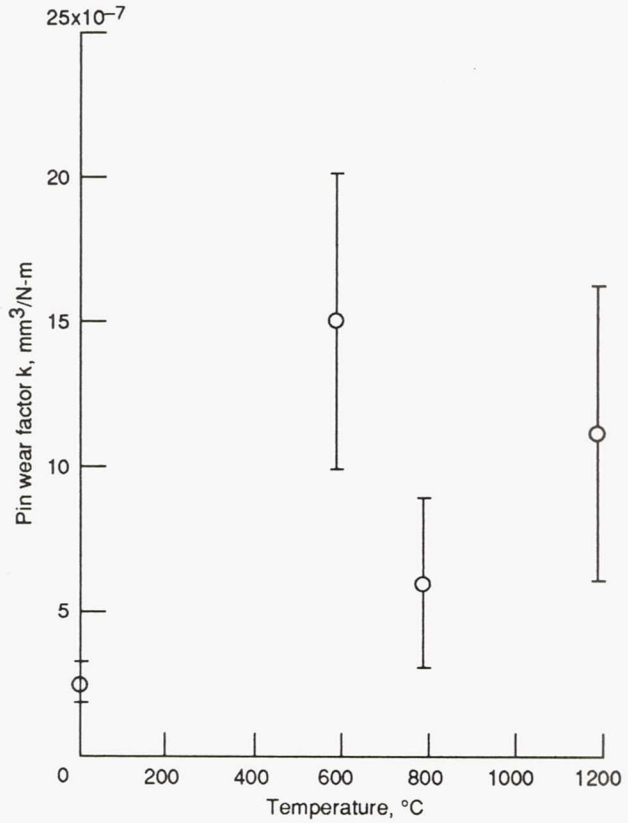

Figure 2.—Plot of the wear factor k (mm^3/Nm) for the Al_2O_3-SiC composite sliding against itself in air at 2.7 m/s, 26 N load [4].

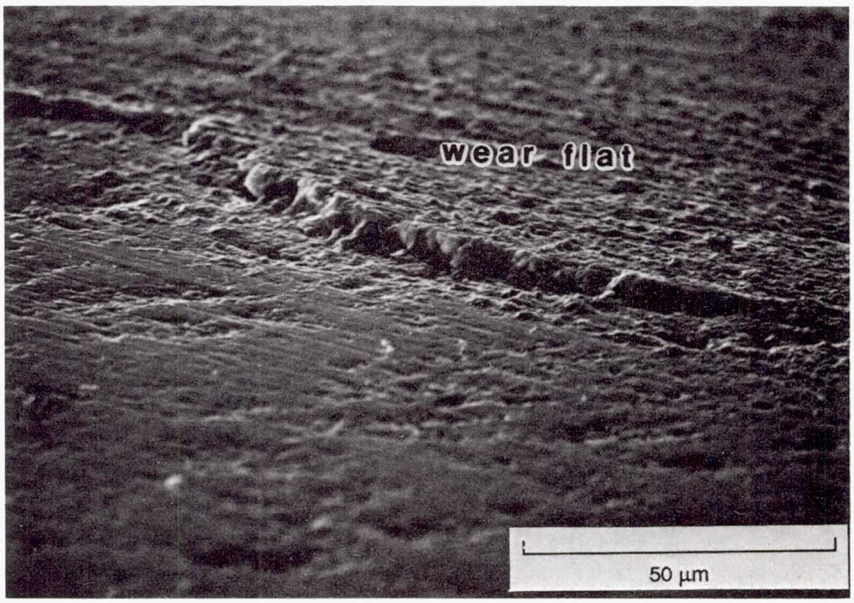

(a)

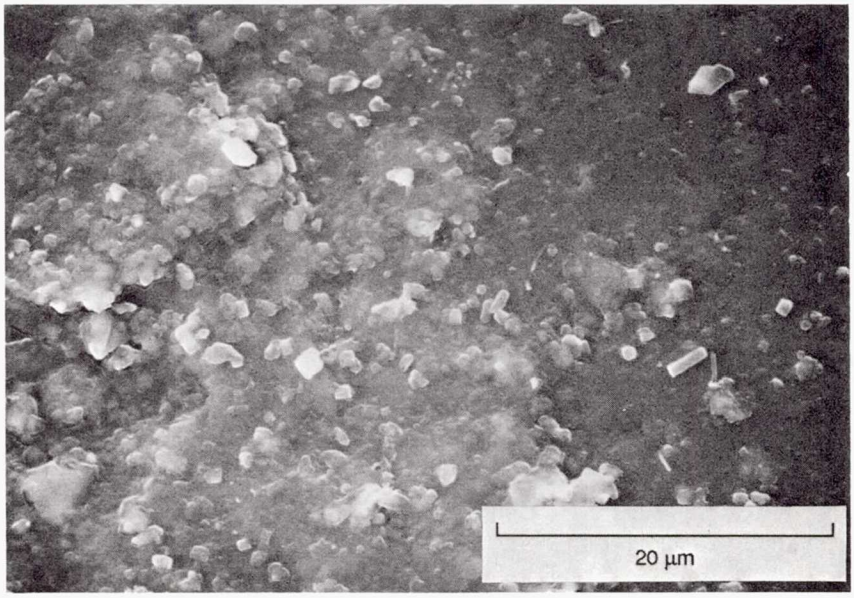

(b)

Figure 3.—(a) Side view of the hemispherical pin showing the ridge of compressed and adherent wear debris (SEM). The center of the wear flat appears in (b). Particles 1 - 3 μm are visible as well as large compacted flakes (lower right). TEM of wear debris reveals much smaller fractured particles 0.2 - 0.5 μm (c).

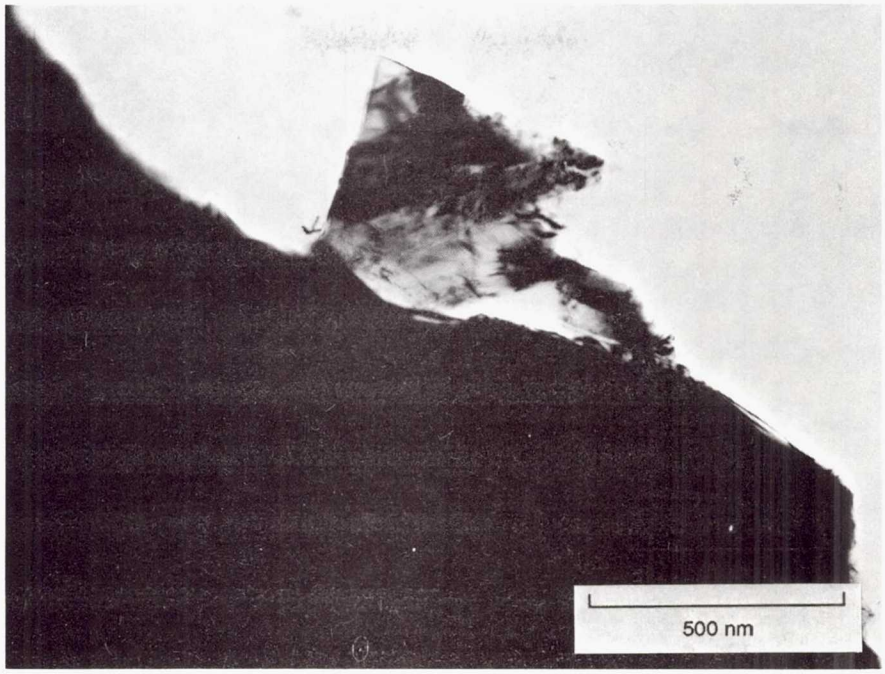

(c)

Figure 3.—Concluded.

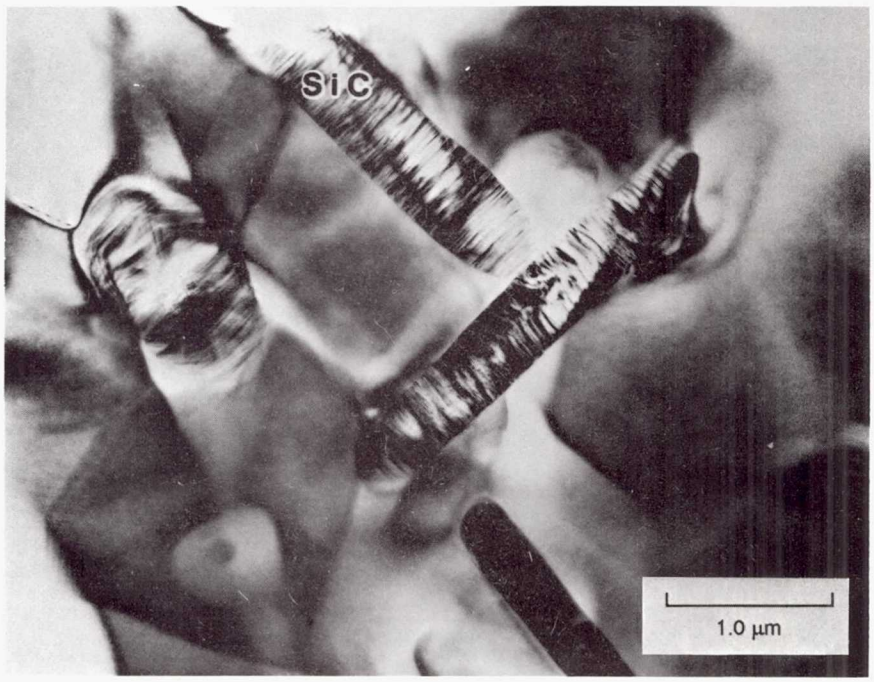

Figure 4.—TEM micrograph of composite pin wear tested at 23 °C. Alumina grains are free of defects. Whiskers exhibit dense stacking faults and impurity inclusions typical of whiskers supplied.

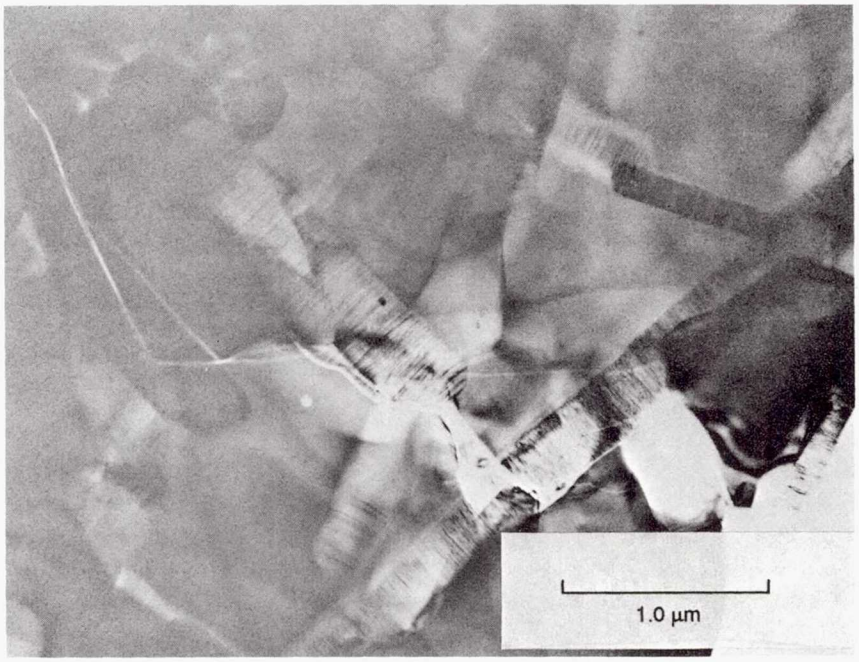

Figure 5.—TEM micrograph of SiC whisker reinforced alumina wear pin. Intra- and intergranular cracking of alumina grains and deflection along whisker itself is evident.

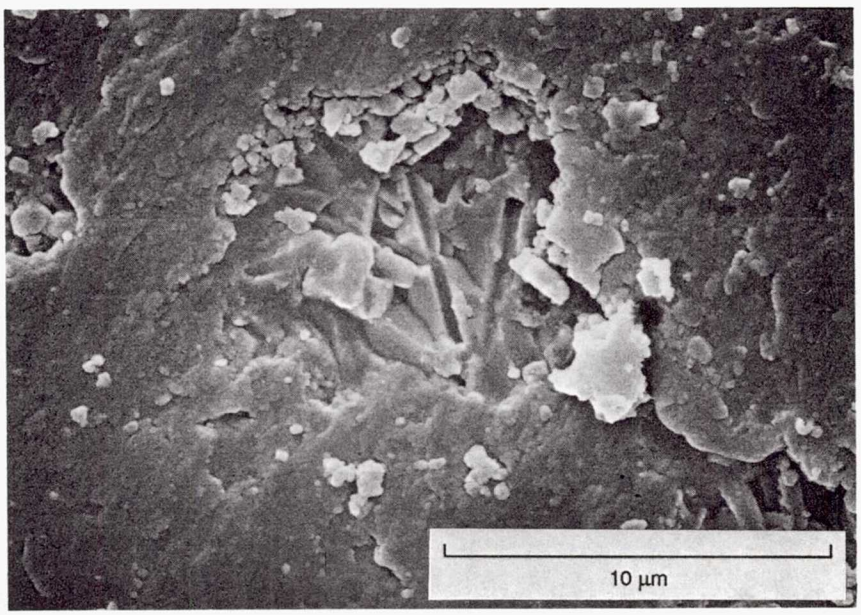

Figure 6.—SEM image of a region of recent massive fracture not yet obscured by compacted debris (600 °C wear). Depressions left by debonded whiskers are visible down the center of massive fracture and to right of center. Debris agglomerates at compacted material surround fracture.

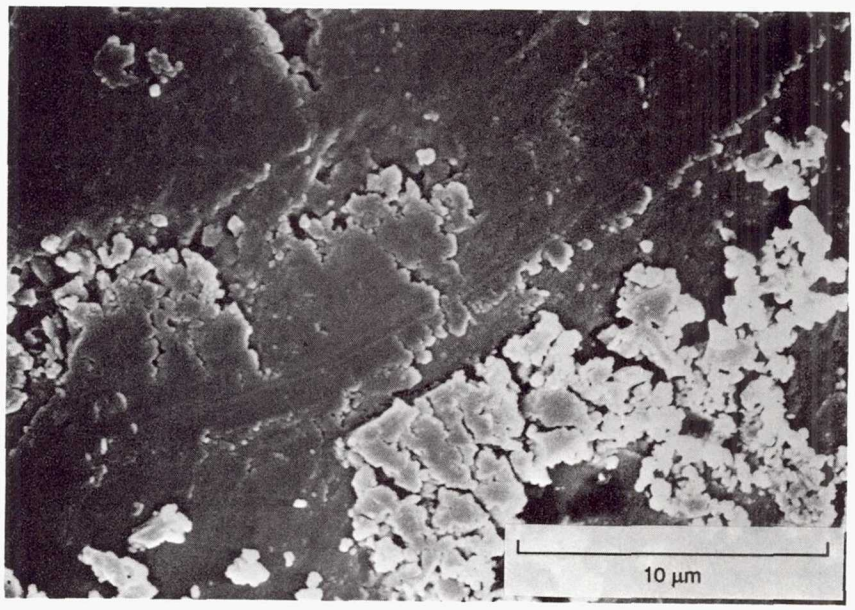

(a)

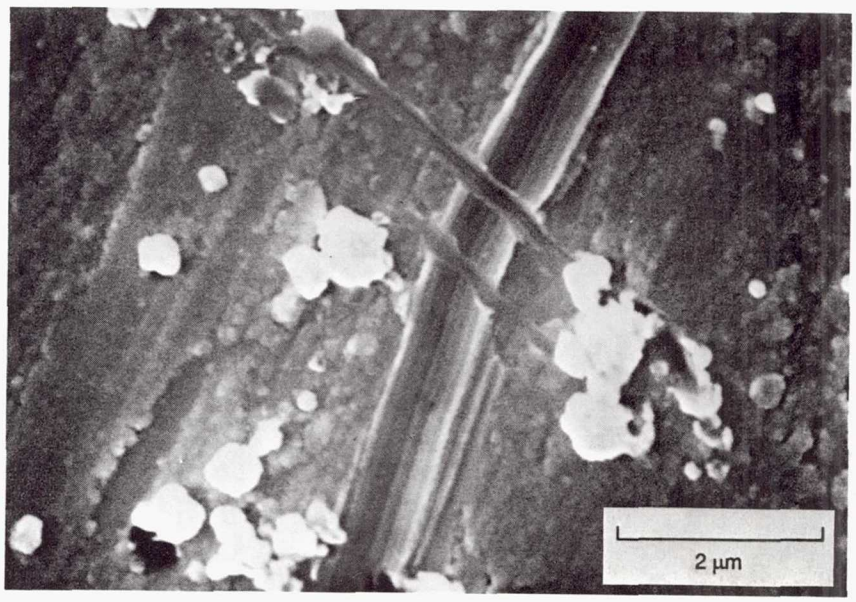

(b)

Figure 7.—(a) SEM image taken near leading edge of sliding surface (600 °C wear) showing initial compaction of debris agglomerates, upper right, and directional smearing of compacted debris to form a thick adherent layer. In (b) the grooving of the adherent layer by debris agglomerates is shown.

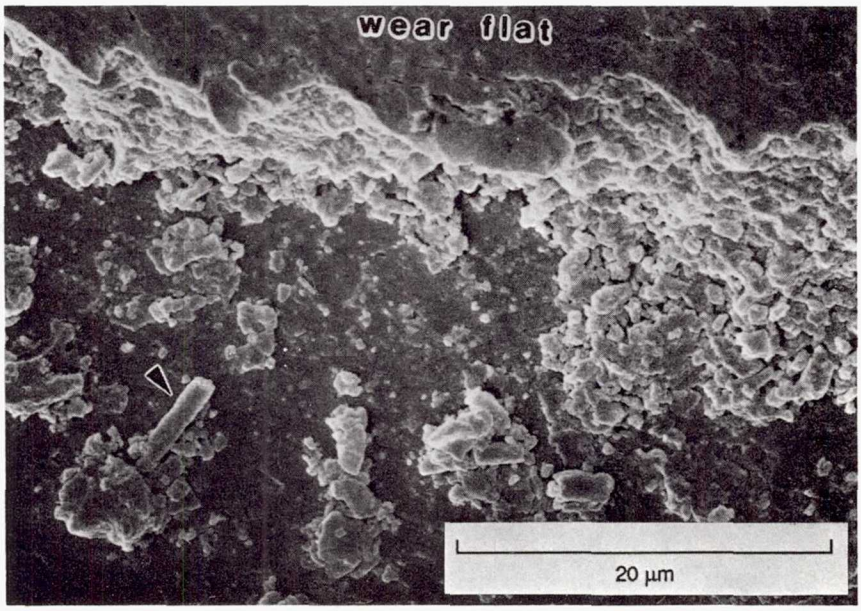

(a)

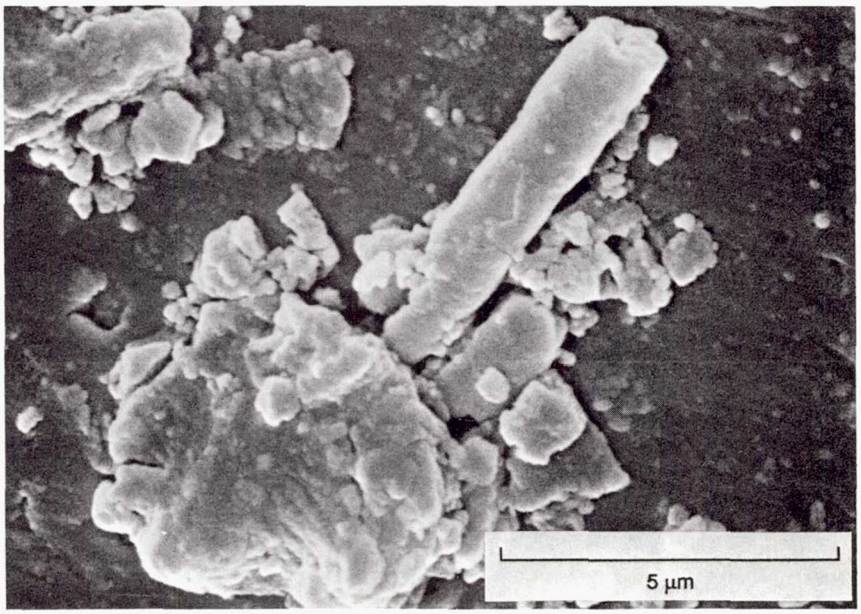

(b)

Figure 8.—(a) SEM image of ridge formed by compacted debris at extremity of 600 °C wear flat. Foreground shows debris particles on machined hemispherical surface. Both very large agglomerates and cylindrical debris are apparent. An enlargement showing an example of cylindrical debris ~ 1 μm dia. EDS analysis of cylindrical debris usually had high Al/Si ratios. It is not clear whether cylindrical debris arise from material adhering to whisker pullouts or occur independently due to mechanical forces in sliding interface.

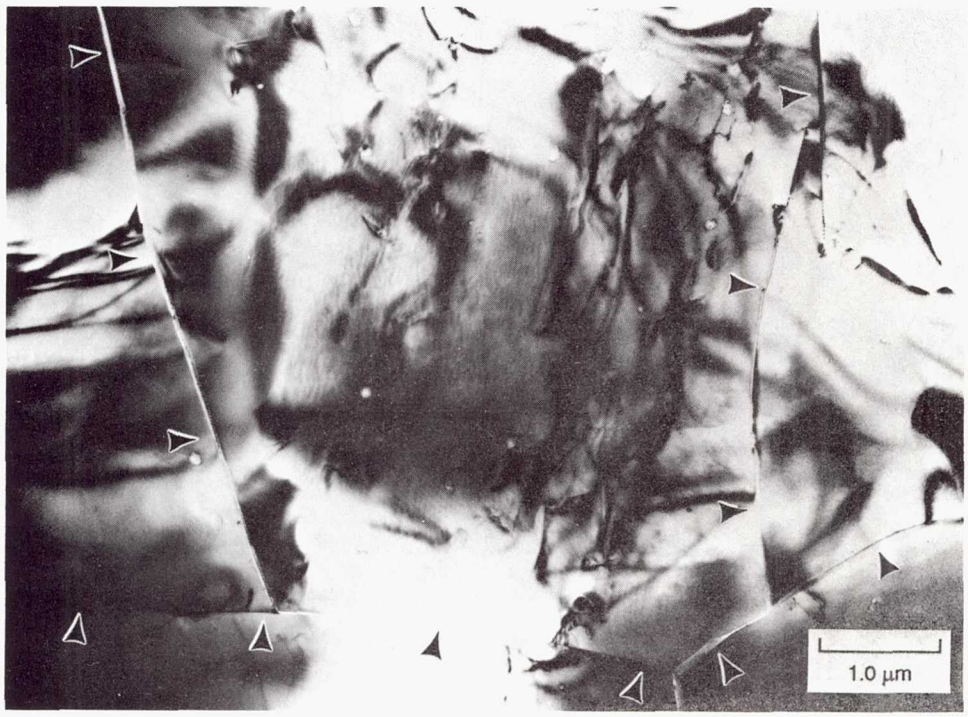

Figure 9.—TEM image of 600 °C wear surface shows extensive microcracking of material. Cracks inclined to surface are not as obvious as those seen "edge on" in micrographs. Arrows have been used to make the full extent of cracking obvious. Dislocations are visible in heavily microcracked regions. Several dislocations are visible in central region of micrograph.

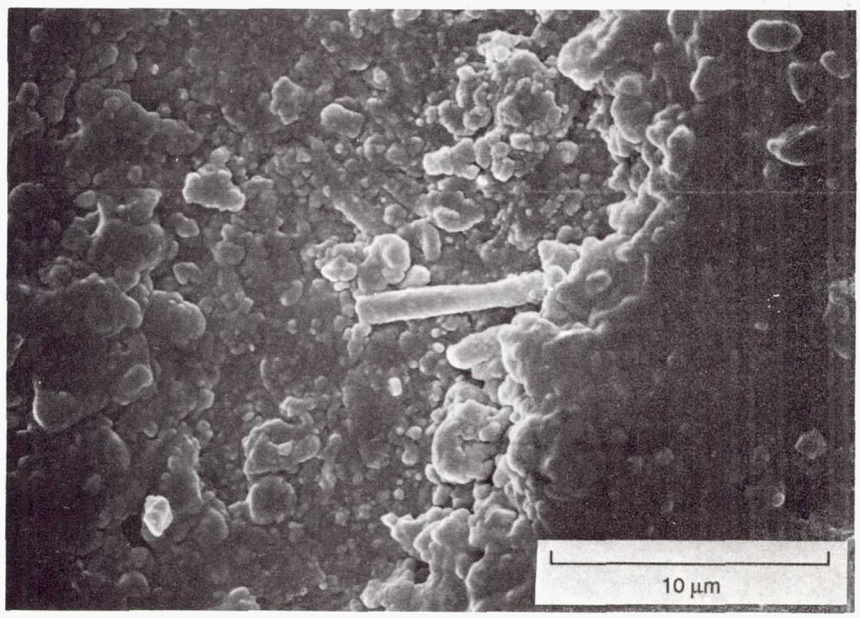

Figure 10.—SEM image of compacted wear debris formed on a pin tested at 800 °C. Larger agglomerates are observed than was seen at lower temperatures. Cylindrical debris is of similar length and diameter as produced at 600 °C.

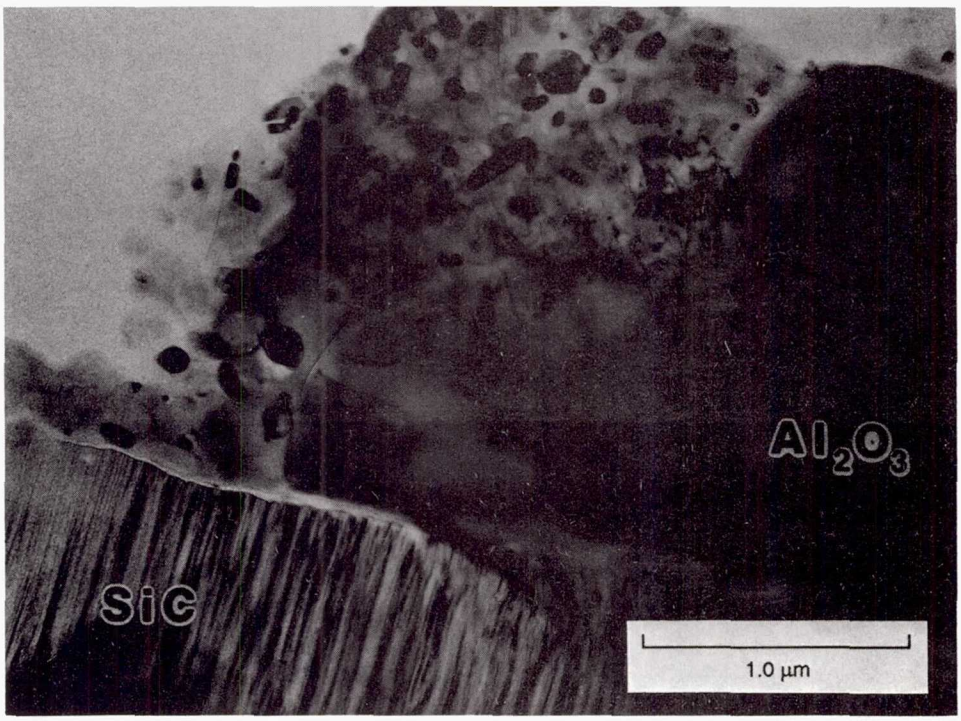

Figure 11.—In TEM images of 800 °C wear surface, mullite crystals ~ 100 nm are dispersed in an alumino-silicate glass (top left). SiC whisker lying in the plane of the foil crosses bottom of micrograph. An alumina grain containing dislocations is seen at right. Several such regions of small mullite crystals were found within the prepared TEM specimen.

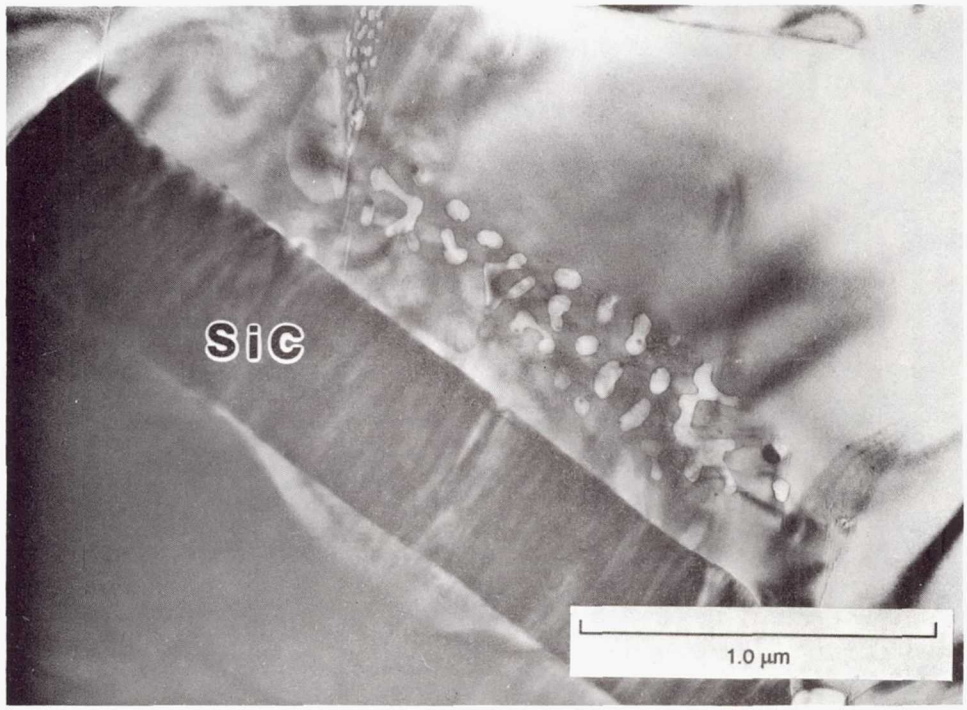

(a)

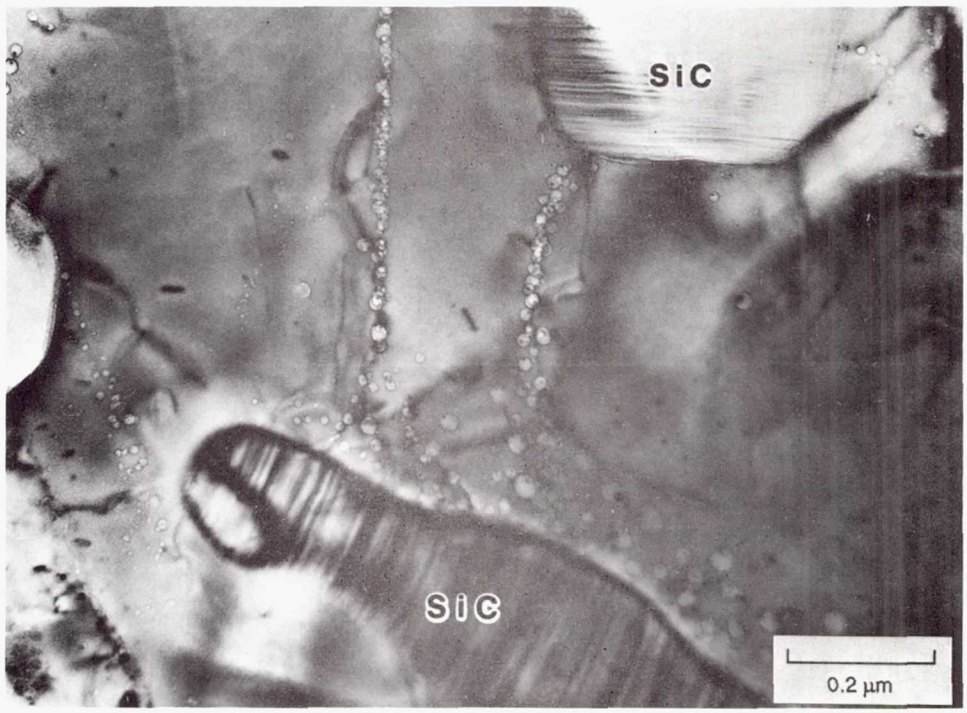

(b)

Figure 12.—TEM image of crack healing captures the crack pinching off to reduce surface area. This is proceeded by ovulation - the breakup (more typically of a cylinder) into a string of spheres. Early stages of this process is shown in (a). The crack will eventually be reduced to a string of pores as seen in (b).

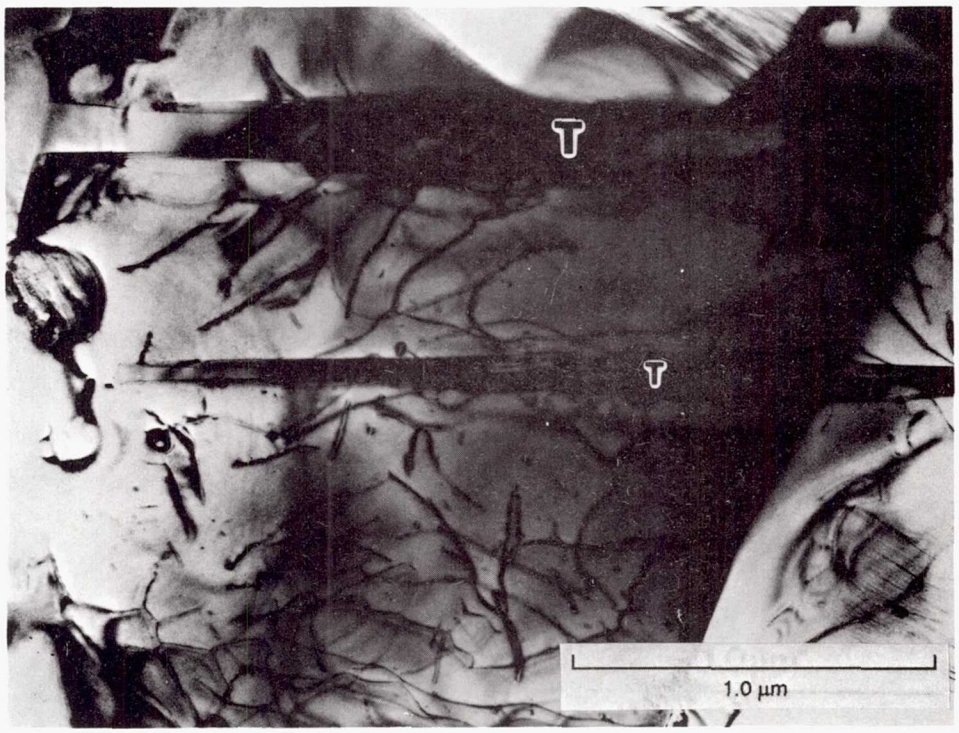

Figure 13.—TEM image of Al_2O_3 grain. Single dislocations and dislocations are visible as well as two twin lathes which extend horizontally across the micrograph (labeled "T").

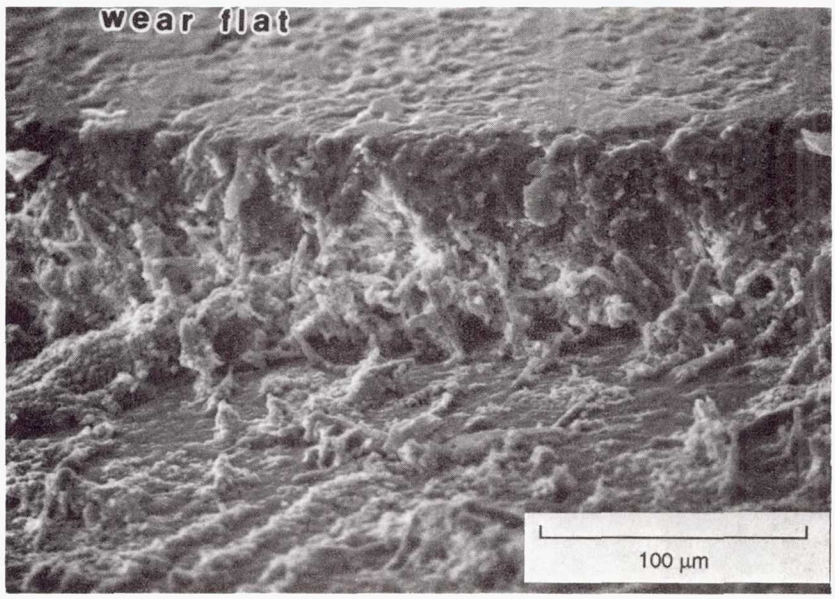

(a)

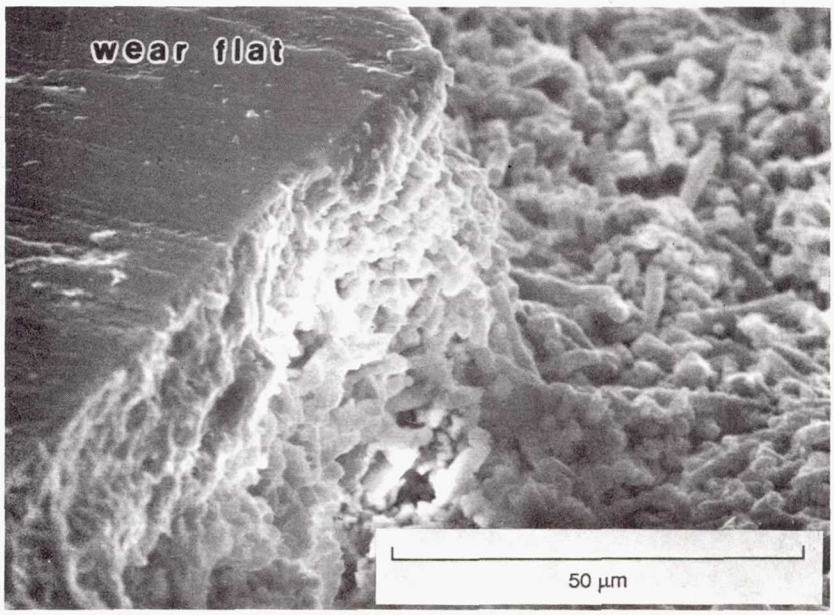

(b)

Figure 14.—(a) SEM micrograph of ridge separating compacted debris from as-machined region of hemispherical pin. Debris is larger than was seen at lower temperatures, being ejected from sliding surfaces before comminution (b). Cylindrical debris up to ~ 55 μm in length and compacted flakes tens of microns in diameter (c) are observed.

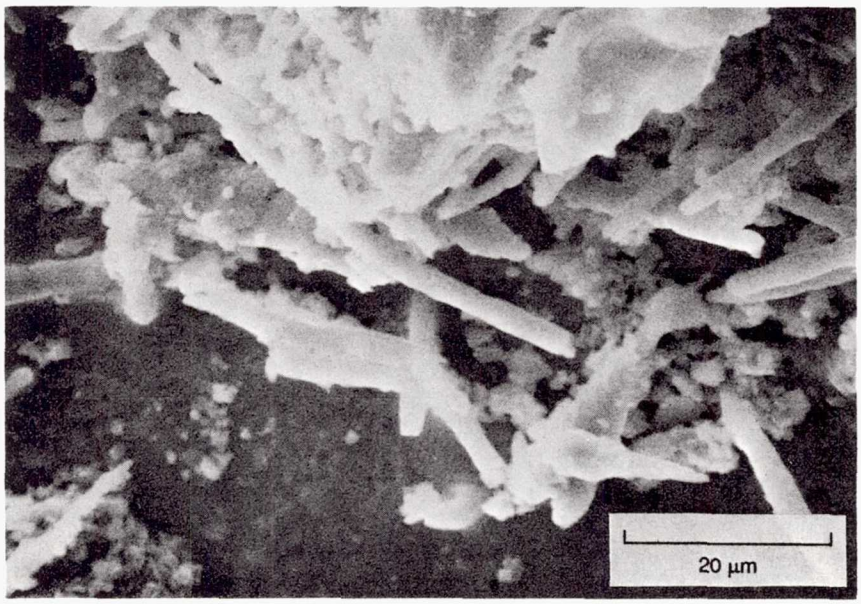

(c)

Figure 14.—Concluded.

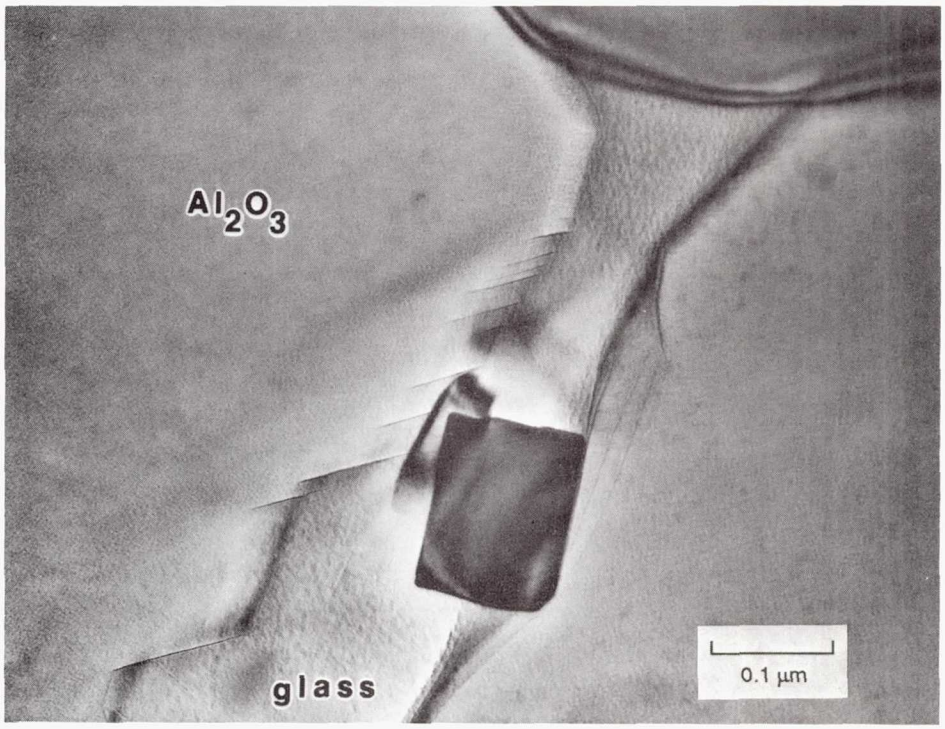

(a)

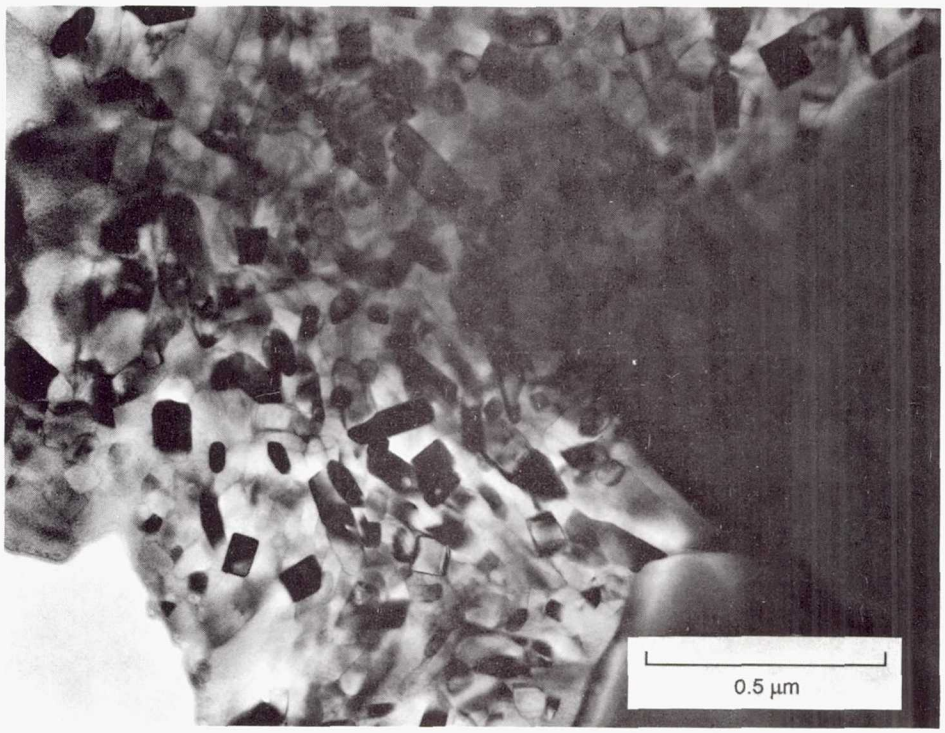

(b)

Figure 15.—(a) TEM image which shows penetration of glass into alumina grain boundaries, faceting of Al_2O_3 grains, and precipitation of mullite. Glass layer is > 100 nm thick. Prismatic mullite crystals precipitate within intergranular glass layer. Mullite is prevalent at wear surface. Regions of mullite plus glass as seen in (b) are typical.

NASA
National Aeronautics and Space Administration

Report Documentation Page

1. Report No.	2. Government Accession No.	3. Recipient's Catalog No.
NASA TM-104490		

4. Title and Subtitle
Sliding Wear of Self-Mated Al_2O_3 - SiC Whisker Reinforced Composites at 23 -1200 °C

5. Report Date
July 1991

6. Performing Organization Code

7. Author(s)
Serene C. Farmer, Patricia O. Book, and Christopher DellaCorte

8. Performing Organization Report No.
E-6344

10. Work Unit No.
505-63-10

9. Performing Organization Name and Address
National Aeronautics and Space Administration
Lewis Research Center
Cleveland, Ohio 44135-3191

11. Contract or Grant No.

13. Type of Report and Period Covered
Technical Memorandum

12. Sponsoring Agency Name and Address
National Aeronautics and Space Administration
Washington, D.C. 20546-0001

14. Sponsoring Agency Code

15. Supplementary Notes
Serene C. Farmer and Christopher DellaCorte, NASA Lewis Research Center; Patricia O. Book, Cleveland State University, Cleveland, Ohio 44115 and Resident Research Associate at NASA Lewis Research Center. Responsible person, Serene C. Farmer (216) 433-3289.

16. Abstract
Microstructural changes occurring during sliding wear of self-mated Al_2O_3-SiC whisker reinforced composites were studied using optical, scanning electron microscopy, and transmission electron microscopy. Pin-on-disk specimens were slid in air at 2.7 m/sec sliding velocity under a 26.5 N load for 1 hr. Wear tests were conducted at 23, 600, 800, and 1200 °C. Mild wear with a wear factor of 2.4×10^{-7} to 1.5×10^{-6} mm^3/Nm was experienced at all test temperatures. The composite shows evidence of wear by fatigue mechanisms at 800 °C and below. Tribochemical reaction (SiC oxidation and reaction of SiO_2 and Al_2O_3) leads to intergranular failure at 1200 °C. Distinct microstructural differences existing at each test temperature are reported.

17. Key Words (Suggested by Author(s))
Wear; Ceramics; High temperature; Aluminum oxides; Whisker composites; Friction; Microstructure

18. Distribution Statement
Unclassified - Unlimited
Subject Category 23

19. Security Classif. (of the report)	20. Security Classif. (of this page)	21. No. of pages	22. Price*
Unclassified	Unclassified	28	A03

NASA FORM 1626 OCT 86

*For sale by the National Technical Information Service, Springfield, Virginia 22161